 © 2008 The Chemical Society of Japan

In Situ Electrochemical Quartz Crystal Microbalance Measurement of Au Deposition and Dissolution in Room-Temperature Ionic Liquid Containing Chloride Ion

Taku Oyama,[1] Takeyoshi Okajima,[1] Takeo Ohsaka,*[1] Shuichiro Yamaguchi,[2] and Noboru Oyama*[2]

[1]Department of Electronic Chemistry, Interdisciplinary Graduate School of Science and Engineering, Tokyo Institute of Technology, 4259-G1-5 Nagatsuta, Midori-ku, Yokohama 226-8502

[2]Department of Applied Chemistry, Graduate School of Science and Technology, Tokyo University of Agriculture and Technology, 2-24-16 Naka-cho, Koganei, Tokyo 184-8588

Received October 29, 2007; E-mail: ohsaka@echem.titech.ac.jp

In-site gold electro-deposition and electro-dissolution have been examined using polycrystalline gold-coated quartz crystal electrode in a room-temperature ionic liquid of 1-ethyl-3-methylimidazolium tetrafluoroborate ($EMIBF_4$). In $EMIBF_4$ media containing 1-ethyl-3-methylimidazolium chloride, the species of Au^I (probably $[Au^ICl_2]^-$) resulting from the electrochemical oxidation of the Au surface was very stable and a reversible voltammetric response of the Au^I/Au^0 couple was observed at 0.25 V vs. Ag wire quasi-reference electrode (Ag(QRE)). In situ electrochemical quartz crystal microbalance (EQCM) technique combined with cyclic voltammetry, double potential-step chronoamperometry and double potential-step chronocoulometry has been successfully applied to investigate the cathodic deposition of Au^I ion to Au metal and the anodic dissolution of Au from the Au electrode surface. It was found that the frequency change of quartz crystal electrode during the electrolysis can be interpreted in terms of rigid mass changes based on the Sauerbrey equation. The EQCM analysis of the electro-dissolution and electro-deposition of Au in the potential range of -0.60 to 0.50 V vs. Ag(QRE) gave the molecular mass equivalent of Au ($197\,g\,mol^{-1}$) corresponding to a one-electron reduction and oxidation of the Au^I/Au^0 redox couple.

Quartz crystal microbalance (QCM) technique has been widely used for micro gravimetric sensing in both gaseous and liquid media over the last two decades.[1–19] Mass loading onto and leaching from the surface of a quartz crystal electrode cause a decrease and an increase, respectively, in the resonant frequency of the oscillator and the frequency change is proportional to the mass change under the condition that there is no viscoelastic change on the electrode surface. Thus, in situ electrochemical QCM (EQCM) technique is one of the best mass-monitoring methods to investigate electrochemical deposition and dissolution of metal ions on electrodes in solutions.

In recent years, room-temperature ionic liquids (RTILs) have become of considerable interest for their potential applications in various areas. Their use in the area of electrochemistry seems also very promising, since extended potential window, decreased electrode passivation, acceptable ionic conductivity, and non-volatility can be advantages gained by their application.[20,21] Therefore, various kinds of RTILs have recently been employed as new media for electrodeposition of metal. The electrodeposition of gold from RTIL was originally reported by Xu and Hussey[22] who examined the electrochemistry of Au^{III} and Au^I at a glassy carbon (GC) electrode in basic aluminum chloride–1-ethyl-3-methylimidazolium chloride ($AlCl_3$–EMICl) ionic liquid and found that the voltammetric reduction of $[Au^{III}Cl_4]^-$ to Au metal occurs in two steps with the intermediate formation of a Au^I complex ($[Au^ICl_2]^-$). Recently, we found that the size and morphology of the Au nanoparticles electrodeposited on GC from EMI tetrafluoroborate (BF_4^-) largely depend on the applied potential (i.e., 0 and -1.0 V).[23] Hardacre et al. have proposed that in electrochemical studies of Au and chloride ion in RTILs the presence of chloride ion, electro-generated trichloride or chlorine is required to enable stripping of deposited Au or electrodissolution of bulk Au.[24] Therefore, EQCM method can be expected to be useful for obtaining a satisfactory interpretation of the reaction mechanisms of Au–halides systems in RTILs.[25–35]

Prior to its use for detecting directly the deposition or dissolution of Au on surfaces, it is necessary to ascertain whether EQCM based on the Sauerbrey equation[4] can be applied essentially as a highly useful technique for quantitatively in situ measuring small mass changes (10^{-9}–10^{-6} g) of electrode surfaces in highly viscous RTILs or not. Undoubtedly the key to succeed in applying this method depends upon the achievement of stable oscillation during an electrochemical reaction process in RTILs. Dai and co-workers have used RTIL as sensing materials for detection of organic vapors based on the usage of QCM for the first time.[18] Very recently, Schäfer et al. have reported that EQCM as vapor sensors, in which 1-*n*-butyl-3-methylimidazolium hexafluorophosphate ($BMIPF_6$) was employed as an adsorption material, provides a stable response of the resonance frequency.[19] Deposition of $BMIPF_6$ on the surface of a quartz electrode induced a negative frequency shift of around 2000 Hz at the crystal with a resonant frequency of 9.95 MHz. Although their measurement is based on an ex situ procedure, the obtained result demonstrates the potential use of in situ EQCM technique in RTILs. One unfavorable

Published on the web June 11, 2008; doi:10.1246/bcsj.81.726

limitation for in situ EQCM measurement in RTILs is that a high viscosity of RTILs induces an undesired overload against oscillation.[36] Higher viscosity of RTIL makes the compensation in a series of oscillation circuits for the higher electro-mechanical impedance of the quartz unfeasible.

In the present paper, we ascertain that the dissolution and deposition of Au in RTIL can give rise to positive and negative frequency shifts, respectively, which obey the Sauerbrey equation[4] indicating a linear relationship between frequency and mass. Previously, it has been found that in $AlCl_3$–EMICl[22] and $EMIBF_4$[23] the electrochemically produced Au^I complex ($[Au^ICl_2]^-$) is obviously very stable. That is to say, we have noticed that the anodic dissolution of the Au electrode as a Au^I ion in $EMIBF_4$ containing chloride anion results in the formation of Au^I chloride complex and the formed complex can be reversibly reduced to Au metal. Therefore, the one-electron reversible redox reaction of this Au^I/Au^0 couple can be expected to be useful to ascertain the principle of the EQCM-based gravimetric method in RTILs, i.e., whether EQCM is applicable or not. The simultaneous measurements of weight change and electric charge would provide a better understanding of the electrode processes of Au deposition and dissolution in RTIL. In the present paper, we also introduce some methods for in situ monitoring a mass change during the electrochemical process, i.e., a differential frequency–potential curve measurement using cyclic voltammetry (CV), a double potential-step chronogravimetric measurement using double potential-step chronocoulometry (DPSCC), and a simultaneous measurement of equivalent molar mass (weight) per second during the potential cycling. Both CV and DPSCC are used for examining whether the proceeding and following reactions between Au^I and Cl^- can contribute to the EQCM responses or not, when the overpotentials ($\eta = E - E^{0\prime}$, where $E^{0\prime}$ is a formal potential) for the oxidation and reduction processes are below or above the potential one for the Tafel region criteria (i.e., $|\eta| \leq$ or > 118 mV at 25 °C).

Experimental

Room-temperature ionic liquid 1-ethyl-3-methylimidazolium tetrafluoroborate ($EMIBF_4$) and EMI chloride (EMICl) were purchased from KANTO Chemicals Co., Japan.

The EQCM is composed of a 6 MHz AT-cut quartz crystal (working electrode area: 1.45 cm^2) which is driven at its resonant frequency by a feedback oscillator.[16] For a 6 MHz crystal operating in the fundamental mode, the approximate sensitivity of the EQCM is 12.3 ng cm^{-2} s, which is an absolute measurement of mass per unit area.[1] Each side of the crystal was coated with Cr (thickness: ca. 2 nm) as an adhesion layer and then with Au (ca. 300 nm) by vacuum deposition with a standard keyhole electrode configuration. One side of the crystal was kept out of the electrolyte solution by using Teflon O-ring. The other side was used as the working electrode. The EQCM measurement was performed in a Faraday cage to eliminate interference from the noise of the surrounding apparatus, particularly a laptop computer. The resonant frequency was measured with a precision of 0.2 Hz.

Electrochemical measurements were carried out in a three-electrode fashion with a potentiostat/galvanostat HZ3000, Hokuto Denko Co., Japan. A Pt wire was used as a counter electrode and a silver wire soaked in $EMIBF_4$ solution in a tube vessel connected to a test solution via a glass frit was used as a quasi-reference electrode. In the EQCM/other electrochemical methods, both frequency and current (or charge) were simultaneously recorded as a function of potential and/or time. Time differentiation of the frequency data and the charge amount was accomplished using the seven points of the individual values,[37] with the Excel slope function of Microsoft®. Potentials are quoted with respect to the Ag wire quasi-reference electrode (Ag(QRE)) and/or the redox potential of the ferrocene/ferricinium ion (Fc/Fc^+) redox couple in $EMIBF_4$, which is 0.12 V vs. Ag(QRE). All the measurements were conducted at room temperature (25 ± 1 °C).

Results and Discussion

Electrochemical Quartz Crystal Microbalance (EQCM)/Cyclic Voltammetry (CV). Figure 1 shows typical cyclic voltammogram obtained at the Au film-coated quartz crystal electrode in $EMIBF_4$ solution in the absence and presence of 8.40 mM (1 M = 1 mol dm^{-3}) EMICl. Also shown in this figure are the frequency–potential responses simultaneously obtained. At first sight, we can see a significant difference in the redox behavior and the frequency–potential responses obtained in the absence and presence of EMICl. In $EMIBF_4$ containing no EMICl, no clear oxidation and reduction currents were observed in the range of potential between −0.60 and 1.80 V, although a reduction wave, probably due to the reduction of impurities (such as H_2O or O_2) dissolved in $EMIBF_4$, was slightly observed around −0.80 V. On the other hand, in the $EMIBF_4$ + EMICl solution, the anodic peak corresponding to the oxidation of the Au was observed at ca. 0.38 V. The oxidation may result in gold dissolution as $[Au^ICl_2]^-$ ion, as judged from the electrochemistry of gold in chloride-containing acid aqueous solutions[25,26] and in RTIL,[22,23]

$$Au^0 + 2Cl^- \rightarrow [Au^ICl_2]^- + e^- \quad (1)$$

A large mass change during the oxidation process, i.e., an increase in frequency can be ascribed to the dissolution of the Au. In this case, the frequency increases with mass loss by oxidation above 0.20 V vs. Ag (QRE). The cathodic peak corresponding to the reduction of $[Au^ICl_2]^-$ species produced during oxidation (eq 1) was observed at ca. 0.15 V. In addition, to be noted is the fact that the frequency change for the oxidation process is much larger than that for the reduction process. In this case, the frequency change does not return exactly to its initial value after the potential cycling, indicating that the deposition–dissolution process of the Au is not completely reversible on the time scale of the potential scan used. At any rate, the frequency–potential response obtained for the Au electrode provides direct evidence for the Au dissolution and deposition during the potential cycling.

Similarly to the CV and EQCM behaviors shown in Figure 1, the clear redox and frequency responses based on the Au/Au^I redox couple were observed in $EMIBF_4$ solution containing EMICl of 1.30–39.7 mM. The shape of the CV resembles that expected for the redox reaction of a solution-phase species that diffuse to the electrode surface. The peak current was found to be proportional to the square root of potential scan rate. Further, it was found that the peak current is also proportional to the concentration of EMICl. This concentration dependence well obeys first-order kinetics. Detailed analysis of the CV behavior obtained will be reported in the

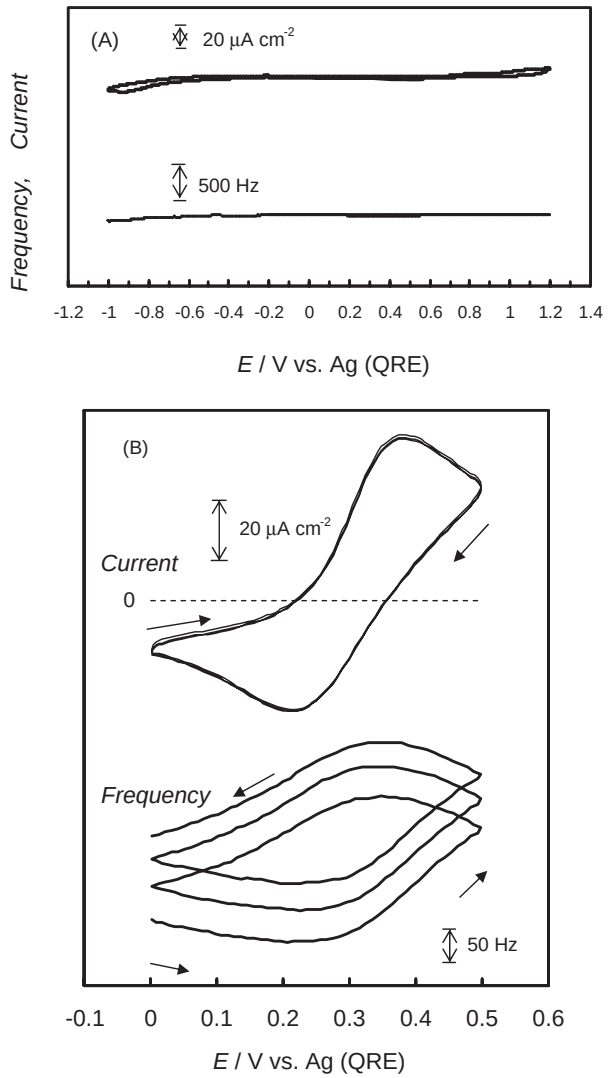

Figure 1. Typical cyclic voltammograms and frequency responses obtained with Au film-coated quartz crystal electrode (area: 1.45 cm^2, film thickness: 300 nm) in containing (A) 0 and (B) 8.40 mM EMICl. The electrode potential was scanned at (A) 5 and (B) 10 mV s^{-1}. In the absence of EMICl, the electrode potential was scanned from the rest potential (ca. 0.20 V vs. Ag(QRE)) to −1.00 V and then from −1.00 to 1.20 V and further from 1.20 V to the initial potential. In the presence of 8.40 mM EMICl, the potential scan was repeated three times in the range of potential between 0 and 0.50 V.

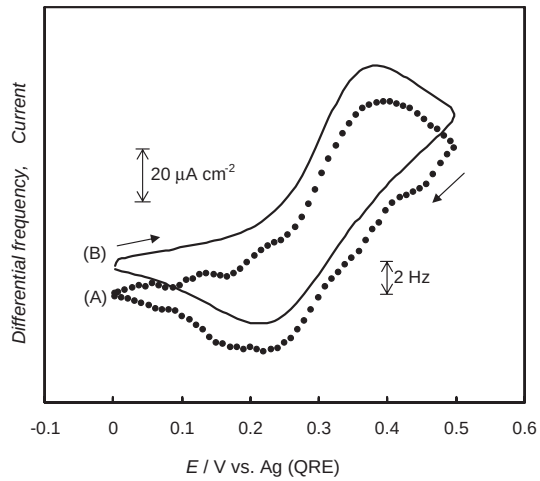

Figure 2. (A) Differential frequency (●) and (B) current (—) responses simultaneously obtained during cyclic voltammetric measurements under the same experimental conditions as those in Figure 1B.

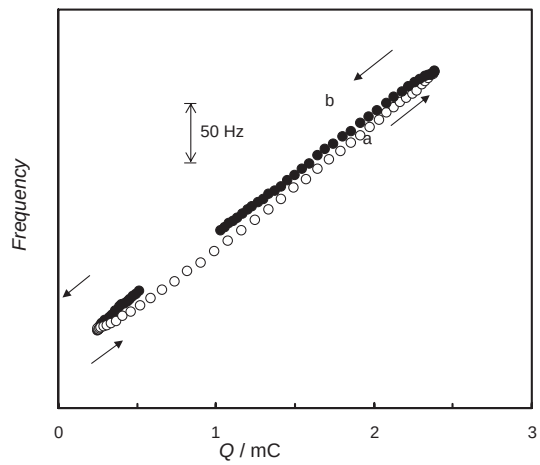

Figure 3. Plots of the frequency change vs. the amount (Q) of charge passed during cyclic voltammetric measurements under the same experimental conditions as those in Figure 1B. The frequency changes (a) (○) and (b) (●) correspond to the oxidation process from 0.21 to 0.50 V and then to 0.36 V, and the reduction process from 0.36 to 0 V and then to 0.21 V, respectively.

near future,[38] where characterization of the Au^I/Au^0 redox couple not only on Au-QCM but also on Pt-QCM electrodes will be performed along with XPS and UV–vis spectroscopic measurements.

To make it clear that the observed CV response is directly correlated with the mass change of the Au electrode surface, we newly introduce the plot of a (df/dt) term (i.e. values of time (t)–differential frequency (f) against the potential, as demonstrated in Figure 2. Here, the values of (df/dt) term were calculated by the least-squares method, which is "Excel slope function of Excel programs (Microsoft®)," using the 7 points of the frequency values measured at back and forth each second.[36] As can be seen from the differential frequency–potential curve (abbreviated as DFPC), the whole shape and the relative magnitude change of the (df/dt) response coincide with those of the current in the potential range of 0 to 0.5 V. The result demonstrates that the current response is simply in harmony with the gravimetric change on the Au electrode surface.

As shown in Figure 3, the dissolution of Au is characterized in the potential range of 0 to 0.5 V, where the amount (Q) of charge passed during the potential sweep is changed from 0.260 to 2.38 mC. The plot of frequency change (Δf) vs. Q yields a straight line. The value of the slope ($\Delta f/Q$) is ca. $(1.57 \pm 0.05) \times 10^{10}$ s^{-1} mol^{-1} cm^2 and thus the value of $\Delta m/Q$ can be estimated as (193 ± 6) g mol^{-1} using the proportionality constant for 6 MHz quartz crystal according to the Sauerbrey equation:

$$\Delta f = -K\Delta m \quad (2)$$

where K is $8.14 \times 10^7\ s^{-1}\ g^{-1}\ cm^2$ for 6 MHz quartz crystal.

This value of $\Delta m/Q$ means that the change in mass of $193\ g\ mol^{-1}$ occurs during the oxidation process. Thus, the observed mass change is simply attributable to the dissolution of Au metal with a Coulomb efficiency of almost 100 percent. The deposition of Au in the reduction is also characterized in the potential range of 0.5 to 0 V, where the amount of Q passed during the potential sweep is varied from 2.38 to 0.990 mC. The plot of Δf vs. Q yields a straight line with the slope of ca. $1.57 \times 10^{10}\ s^{-1}\ mol^{-1}\ cm^2$, which corresponds to $193\ g\ mol^{-1}$. The equivalent mass change obtained during the reduction is just the same as that obtained during the oxidation in the potential range of 0 to +0.5 V.

To display the simultaneous response of mass change with time during the potential scan, we introduce a predicted equivalent mass calculated from the ratio of the observed mass change (Δm) per second to the change of the charge amount (ΔQ) per second during the potential scan,

$$\lambda = nFA(\Delta m/\Delta Q) \quad (3)$$

where λ is the equivalent molar mass (weight), n is the electrodeposition valency, A is the area of electrode surface ($1.45\ cm^2$), and F is the Faraday constant. The values of Δm and ΔQ were evaluated using the seven points observed per second with the Excel slope function of Microsoft®. For the calculation of λ, the value of n is assumed as 1. Figure 4 demonstrates the plot of λ as a function of the electrode potential (E) during the potential cycling. The values of λ per second are in the range of about 175 to 220 g for gold deposition in the potential range 0.25 to 0 V, while they are in the range of about 170 to 200 g for gold dissolution in the potential range 0.35 to 0.5 V. As can be seen from Figure 4, the values of λ are largely scattered in the potential region of 0.25 to 0.35 V, in which faradaic current is flowing with the beginning or ending of oxidation or reduction.

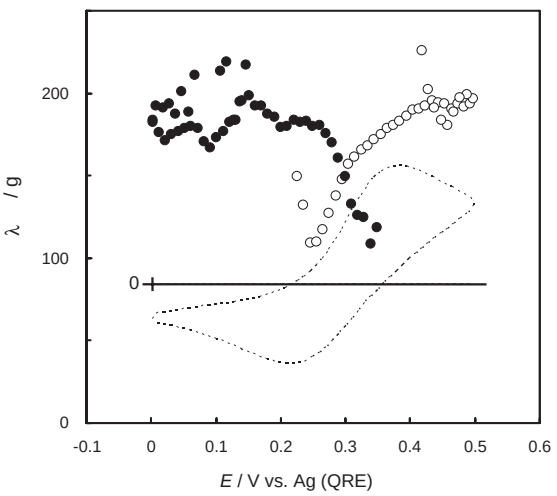

Figure 4. Typical responses (○: for the oxidation, ●: for the reduction) of the equivalent mass (λ), which is defined by eq 3, obtained during cyclic voltammetric measurements (twice) under the same experimental conditions as those in Figure 1B. The dotted CV which is the same as Figure 2A is also shown for comparison.

At relatively high concentrations of EMICl, the values of $\Delta m/Q$ were estimated as less than $197\ g\ mol^{-1}$. As shown in Figure 5, at the concentration of 39.7 mM EMICl, the values of $\Delta m/Q$ during the oxidation and reduction processes were 190 and $175\ g\ mol^{-1}$, respectively. The mass change for the deposition of gold during the negative-direction potential scan was slightly lower than that for the dissolution of gold during the positive-direction potential scan. A partial loss of mass gain during the reduction can be considered due to the following two possible reasons. That is, deficiency in adhesiveness of gold weakly deposited on the electrode surface may result in the subsequent physical loss of gold atoms on the surface, where a large amount of deposition may induce restructuring of the gold on the surface.[37,39–42] As another possible reason we consider that the following disproportionation process (eq 4) could slightly contribute to the re-deposition of Au.

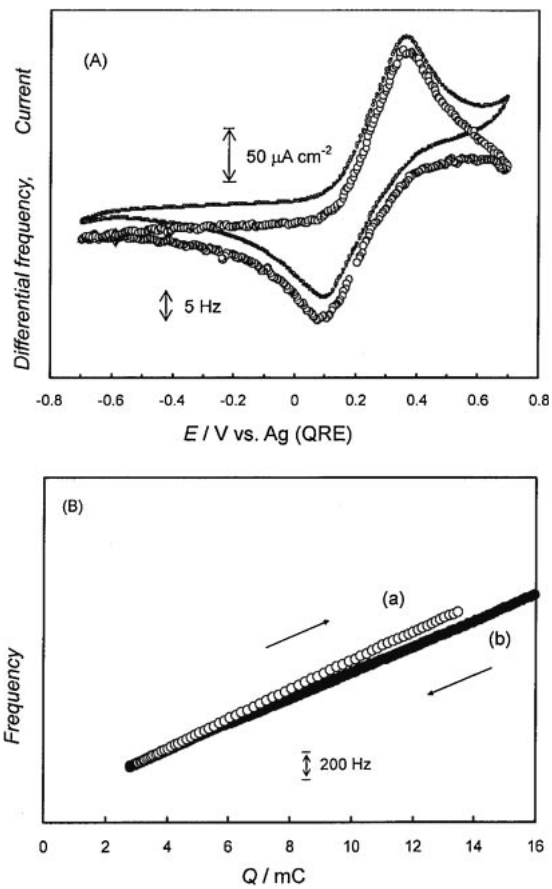

Figure 5. (A) Differential frequency (○) and current (—) responses simultaneously obtained during cyclic voltammetric measurements with Au film-coated quartz crystal electrode (area: $1.45\ cm^2$, film thickness: 300 nm) in the potential range between −0.70 and 0.70 V at a potential scan of $5\ mV\ s^{-1}$ in $EMIBF_4$ containing 39.7 mM EMICl. (B) Plots of the frequency change vs. the amount (Q) of charge passed during cyclic voltammetric measurements. The frequency changes (a) (○) and (b) (●) correspond to the oxidation from 0.25 to 0.70 V and the reduction from 0.70 to −0.70 V, respectively.

$$3[Au^{I}Cl_2]^- = 2Au^0 + [Au^{III}Cl_4]^- + 2Cl^- \quad (4)$$

Above 0.60 V, a second rise in the oxidation current was observed as shown in Figure 5A, but the value of (df/dt) continued to decline. This means that a part of the observed oxidation current is associated with the oxidation reaction which is not accompanied by a weight loss, possibly the oxidation of Au^I chloride complex to Au^{III} complex or the oxidation of chloride.[24] Related experiments are now in progress and the results will be reported in the near future.[38]

Electrochemical Quartz Crystal Microbalance/Double Potential-Step Chronoamperometry and Double Potential-Step Chronocoulometry. Here, in order to simplify the redox process (eq 1), which would include various elementary reactions, the applied step-potentials in the measurements using double potential-step (DPS) methods were fixed above the potential based on the Tafel region criteria. Figure 6 demonstrates typical current, charge, and frequency responses as a function of time obtained for DPS measurements[38] with a gold film-coated quartz crystal electrode in $EMIBF_4$ containing 8.40 mM EMICl. In this case, the potential of the Au electrode was stepped from 0.25 (the rest potential at the present working electrode) to 0.50 V, at which the oxidation of Au actually occurs (see the cyclic voltammogram shown in Figure 1B), and then stepped from 0.50 to −0.60 V, at which the reduction of Au^I complex ions takes place. When the potential is stepped from 0.25 to 0.50 V, the anodic current flows and at the same time the frequency increases gradually with increasing electrolysis time. On the other hand, when the potential is stepped from 0.50 to −0.60 V, the frequency decreases gradually as the cathodic current flows. This can be, on the whole, expected from the fact that the oxidation process is ascribed to the dissolution of the Au and the reduction process corresponds to the reduction of Au^I complex ions produced during the oxidation process, as expressed by eq 1. Here, we can point out the fact that the plots of Δf vs. Q for both the oxidation and reduction processes yield straight lines with almost the same slopes (see Figure 7), suggesting that the same redox couple is associated with the mass change (Δm) of the Au electrode during both the oxidation and reduction processes. The value of the slope $(\Delta f/Q)$ is ca. $(1.61 \pm 0.05) \times 10^{10}\,s^{-1}\,mol^{-1}\,cm^2$ and thus the value of $\Delta m/Q$ can be estimated to be $(198 \pm 6)\,g\,mol^{-1}$ using the proportionality constant between Δf and Δm. This evaluated value of $\Delta m/Q$ means that the change in mass of $198\,g\,mol^{-1}$ of electroactive species occurs during the oxidation–reduction process. Thus, the observed mass change is simply attributable to the dissolution and deposition of the Au^I/Au^0 redox couple, because the atomic weight of Au is 196.97 g. Thus, DPS measurement combined with a quartz crystal microbalance on the electrochemical dissolution and deposition of the Au^I/Au^0 redox couple with a gold film-coated quartz crystal electrode in $EMIBF_4$ containing EMICl proved to be highly useful in ascertaining EQCM predictions based on the Sauerbrey equation.

It is worth while to note that the dissolution and deposition efficiencies of the Au^I/Au^0 redox couple were about 100%, which can be regarded as the theoretical value, for the DPS method. The clear discrepancy in the obtained efficiencies between the DPS and CV measurements was not observed. Therefore, under the present experimental conditions, it can be concluded that the contributions of the kinetics of disproportionation (eq 4), double layer charging during potential-sweep or potential-step, the proceeding or following reactions between Au^I and Cl^-, and so on to EQCM responses are almost negligible.

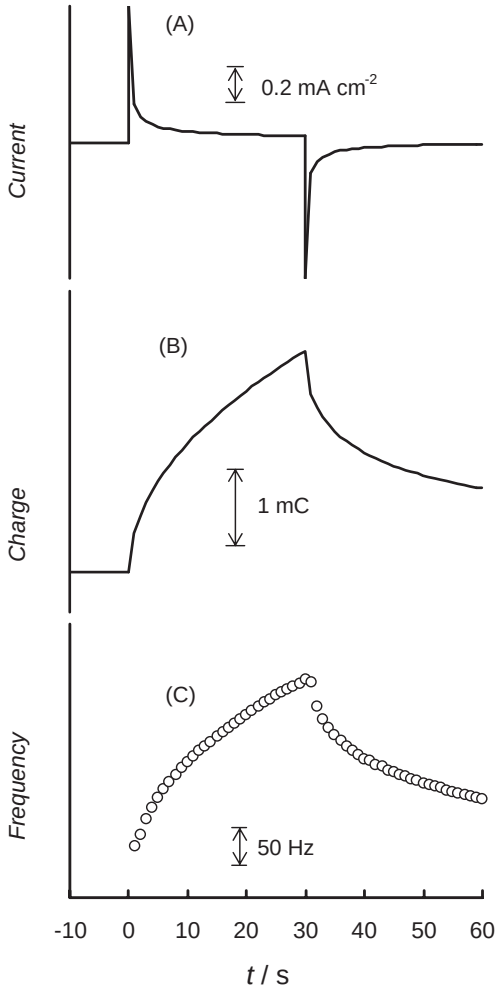

Figure 6. Typical current, charge, and frequency responses as a function of time obtained for double potential-step chronoamperometric and chronocoulometric measurements with Au film-coated quartz crystal electrode (area: 1.45 cm^2, thickness: 300 nm) in $EMIBF_4$ containing 8.40 mM EMICl. (A): Current response; (B): charge response; and (C): frequency response. The potential was stepped from 0.25 to 0.50 V (for 30 s) and then from 0.50 to −0.60 V (for 30 s).

Conclusion

It has been demonstrated that electrochemical quartz crystal microbalance (EQCM) can be employed as a highly sensitive in situ probe of changes in mass of electrode surfaces in RTILs. The redox reaction of Au film-coated electrode in $EMIBF_4$ containing chloride ion is introduced to ascertain the principle of gravimetric methods based on EQCM. The coulomb efficiency of almost 100% for the dissolution and deposition of Au is obtained for the EQCM responses in the cyclic voltammetric and the double potential-step chronoamperometric measurements.

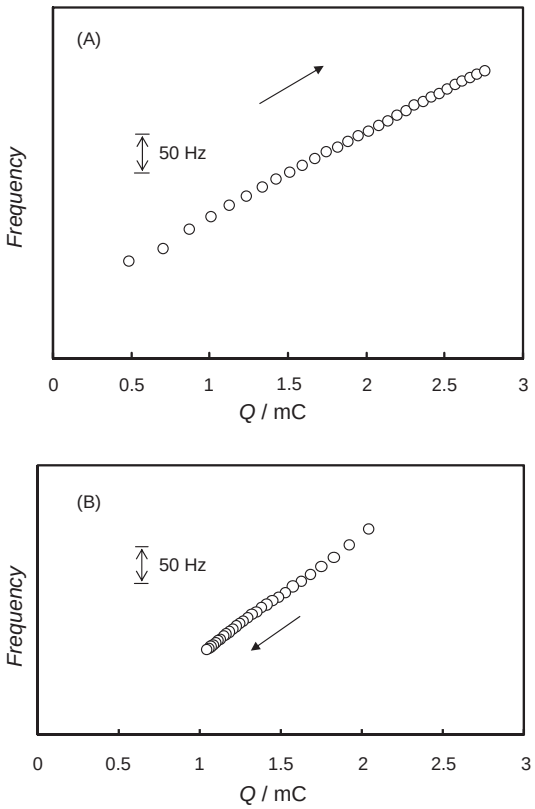

Figure 7. Plots of the frequency change vs. the amount (Q) of charge passed for the forward potential-step (A: oxidation) and the reverse potential-step (B: reduction) at Au film-coated quartz crystal electrode. The data were taken from Figure 6.

The present work was financially supported by Grant-in-Aid for Scientific Research (A) (No. 19206079) from the Ministry of Education, Culture, Sports, Science and Technology (MEXT), Japan.

References

1 C. Lu, A. W. Czanderna, *Applications of Piezoelectric Quartz Crystal Microbalances*, Elsevier Science, **1984**.

2 J. Janata, *Principles of Chemical Sensors*, Plenum Press, **1989**, p. 55.

3 M. R. Deakin, D. A. Buttry, *Anal. Chem.* **1989**, *61*, 1147A.

4 G. Sauerbrey, *Z. Phys.* **1959**, *155*, 206.

5 S. Bruckenstein, M. Shay, *J. Electroanal. Chem.* **1985**, *188*, 131.

6 M. R. Deakin, T. T. Li, O. R. Melroy, *J. Electroanal. Chem.* **1988**, *243*, 343.

7 M. R. Deakin, O. R. Melroy, *J. Electroanal. Chem.* **1988**, *239*, 321.

8 M. Mizunuma, T. Ohsaka, H. Miyamoto, N. Oyama, *Bull. Chem. Soc. Jpn.* **1991**, *64*, 2887.

9 S. J. Lasky, D. A. Buttry, *J. Am. Chem. Soc.* **1988**, *110*, 6258.

10 H. Masuda, T. Yoshino, K. Arai, N. Baba, *Chem. Lett.* **1988**, 1337.

11 D. Orata, D. A. Buttry, *J. Am. Chem. Soc.* **1987**, *109*, 3574.

12 H. Daifuku, T. Kawagoe, N. Yamamoto, T. Ohsaka, N. Oyama, *J. Electroanal. Chem.* **1989**, *274*, 313.

13 N. Oyama, N. Yamamoto, O. Hatozaki, T. Ohsaka, *Jpn. J. Appl. Phys.* **1990**, *29*, L818.

14 M. W. Carr, A. R. Hillman, S. D. Lubetkin, M. J. Swwan, *J. Electroanal. Chem.* **1989**, *267*, 313.

15 N. Yamamoto, T. Ohsaka, T. Terashima, N. Oyama, *J. Electroanal. Chem.* **1990**, *296*, 463.

16 a) T. Okajima, H. Sakurai, N. Oyama, K. Tokuda, T. Ohsaka, *Bull. Chem. Soc. Jpn.* **1992**, *65*, 1884. b) N. Yamamoto, T. Yamane, T. Tatsuma, N. Oyama, *Bull. Chem. Soc. Jpn.* **1995**, *68*, 1641.

17 H. D. Liess, A. Knezevic, M. Rother, J. Muenz, *Faraday Discuss.* **1997**, *107*, 39.

18 C. Liang, C.-Y. Yuan, R. J. Warmack, C. E. Barnes, S. Dai, *Anal. Chem.* **2002**, *74*, 2172.

19 T. Schäfer, F. D. Francesco, R. Fuoco, *Microchem. J.* **2007**, *85*, 52.

20 J. S. Wilkes, J. A. Levisky, R. A. Wilson, C. L. Hussey, *Inorg. Chem.* **1982**, *21*, 1263.

21 H. I. Chum, R. A. Osteryoung, in *Ionic Liquids*, ed. by D. Inman, D. G. Lovering, Plenum Press, New York, **1981**, pp. 407–423.

22 X. H. Xu, C. L. Hussey, *J. Electrochem. Soc.* **1992**, *139*, 3103.

23 T. Oyama, T. Okajima, T. Ohsaka, *J. Electrochem. Soc.* **2007**, *154*, D322.

24 a) L. Aldous, D. S. Silvester, C. Villagran, W. R. Pitner, R. G. Compton, M. C. Lagunas, C. Hardacre, *New J. Chem.* **2006**, *30*, 1576. b) C. Villagran, C. E. Banks, C. Hardacre, R. G. Compton, *Anal. Chem.* **2004**, *76*, 1998.

25 G. H. Kelsall, N. J. Welham, M. A. Diaz, *J. Electroanal. Chem.* **1993**, *361*, 13.

26 M. A. Diaz, G. H. Kelsall, N. J. Welham, *J. Electroanal. Chem.* **1993**, *361*, 25.

27 F. A. Cotton, G. Wilkinson, *Advanced Inorganic Chemistry*, 5th ed., Wiley, New York, **1988**, pp. 946–951.

28 J. J. Lingane, *J. Electroanal. Chem.* **1962**, *4*, 332.

29 D. H. Evans, J. J. Lingane, *J. Electroanal. Chem.* **1964**, *8*, 173.

30 A. D. Goolsby, D. T. Sawyer, *Anal. Chem.* **1968**, *40*, 1978.

31 G. Delarue, *J. Electroanal. Chem.* **1960**, *1*, 285.

32 H. A. Laitinen, C. H. Liu, *J. Am. Chem. Soc.* **1958**, *80*, 1015.

33 R. Combes, J. Vedel, B. Tremillon, *J. Electroanal. Chem.* **1970**, *27*, 174.

34 H. C. Gaur, H. L. Jindal, *Electrochim. Acta* **1970**, *15*, 1113.

35 U. Anders, J. A. Plambeck, *Can. J. Chem.* **1969**, *47*, 3055.

36 Since in general, RTIL has higher viscosity (by one–two orders of magnitude) than that of conventional solvents, as can be readily seen from the comparison of the viscosities of $EMIBF_4$ and H_2O (27 and 1.0 mPa s), the value of the resistance component for an electro-mechanical impedance of the quartz crystal electrode in RTIL is increased, and consequently compensation in oscillation circuit for the resulting resistance becomes increasingly difficult. Thus, the oscillation is apt to be unsteadied or stopped by overload and/or coupling with the impedance of the electrical circuits for measurement composed of potentiostat/galvanostat and laptop computer. Even if stable oscillation is gained, we need to confirm whether frequency changes are interpreted in terms of rigid mass changes or not. The most appropriate experiment to prove the hypothesis of rigid mass change is the electro-deposition of metal ion. Previously, we have reported that by means of ex situ quartz crystal impedance (QCI) technique measuring the suscep-

tance–conductance spectra,[16a] in situ EQCM technique and in situ EQCI technique, that hypothesis holds for the EQCM monitoring of metal deposition.[16b]

37 A. Savitzky, M. J. E. Golay, *Anal. Chem.* **1964**, *36*, 1627.

38 T. Oyama, T. Okajima, T. Ohsaka, S. Yamaguchi, N. Oyama, to be submitted.

39 O. M. Magnussen, J. Hotlos, R. J. Behm, N. Batina, D. M. Kolb, *Surf. Sci.* **1993**, *296*, 310.

40 A. J. Bard, H. D. Abruna, C. E. Chidsey, L. R. Faulkner, S. W. Feldberg, K. Itaya, M. Melroy, O. Mejda, R. W. Murray, M. D. Porter, M. P. Soriaga, H. S. White, *J. Phys. Chem.* **1993**, *97*, 7147.

41 X. Gao, G. J. Edens, A. Hamelin, M. J. Weaver, *Surf. Sci.* **1994**, *318*, 1.

42 D. T. Sawyer, J. S. Valentine, *Acc. Chem. Res.* **1981**, *14*, 393.

43 F. C. Anson, *Anal. Chem.* **1966**, *38*, 54.